Journal of Applied Polymer Science

In situ synthesis of biopolyurethane nanocomposites reinforced with modified multiwalled carbon nanotubes

Chaoqun Zhang,[1] Danny Vennerberg,[1] Michael R. Kessler[2]
[1]Department of Materials Science and Engineering, Iowa State University, Ames, Iowa
[2]School of Mechanical and Materials Engineering, Washington State University, Pullman, Washington
Correspondence to: M. R. Kessler (E-mail: MichaelR.Kessler@wsu.edu)

ABSTRACT: Biopolyurethane nanocomposites reinforced with silane-modified multiwalled carbon nanotubes (s-MWCNT) were successfully prepared. The carbon nanotube surfaces were modified by means of functional amine groups via ozone oxidation followed by silanization. The surface structure of the s-MWCNTs was characterized by Fourier transform infrared spectroscopy, X-ray photoelectron spectroscopy, and thermogravimetric analysis. The s-MWCNTs were incorporated into a vegetable oil-based polyurethane (PU) network via covalent bonding to prepare PU nanocomposites. The effect of s-MWCNT loading on the morphology, thermomechanical, and tensile properties of the PU nanocomposites was studied. It was determined that the s-MWCNTs were dispersed effectively in the polymer matrix and that they improved the interfacial strength between the reinforcing nanotubes and the polymer matrix. Storage modulus, glass transition temperature, Young's modulus, and tensile strength of the nanocomposites increased with increasing s-MWCNT loading up to 0.8%. However, increasing the s-MWCNT content to 1.2 wt % resulted in a decrease in thermomechanical properties of the PU nanocomposites. This effect was attributed to the fact that at high s-MWCNT contents, the increased number of amine groups competed with the polyol's hydroxyl groups for isocyanate groups, causing a decrease in the integrity of the PU matrix. High s-MWCNT contents also facilitated aggregation of the nanotubes, causing a decrease in thermomechanical properties. © 2015 Wiley Periodicals, Inc. J. Appl. Polym. Sci. **2015**, *132*, 42515.

KEYWORDS: composites; mechanical properties; polyurethanes

Received 25 January 2015; accepted 18 May 2015
DOI: 10.1002/app.42515

INTRODUCTION

Polyurethane (PU) is one of the most versatile polymeric materials; it exhibits excellent properties[1–3] and is therefore widely used in a variety of applications, including coatings, adhesives, foams, and sealants.[4,5] A common approach to expand its range of applications is to tailor the properties of PU to meet the performance needs of a given application. This can be achieved by controlling the selection of the starting materials (polyols, isocyanates, chain extender) and their ratios.

Vegetable oil-based polyols have gained increasing attention worldwide as sustainable building blocks that can partially or completely substitute for their fossil fuel counterparts.[6–8] The structure–property relationships between these novel polyols and the resulting PUs have been extensively investigated. The hydrophobic triglyceride structure of vegetable oils greatly enhances the final physical and thermomechanical properties of PU.[9,10] Guo reported that rigid PU foams prepared from methoxylated soybean oil polyol exhibited comparable mechanical and insulating properties, with their thermal resistance superior, to those from petrochemical feedstock.[11] Glass-reinforced PU composites using Soypolyol 204 derived from soybean oil showed better oxidative and hydrolytic stability than their petrochemical equivalents.[12]

Another strategy to improve the mechanical, thermal, and electrical properties of PU is to incorporate functional fillers or fibers into the matrix. For example, short banana leaf fibers were used to improve the tensile strength and dynamic mechanical properties of vegetable oil-based PUs.[13,14] The incorporation of long glass fibers improved the physicomechanical properties and thermal stability of biobased PUs.[15] Attapulgite particles were incorporated in a PU matrix to prepare porous materials that exhibit strong dye adsorption capabilities for waste water treatment.[16]

The use of carbon nanotubes as reinforcements in various matrices has been extensively investigated. They offer high aspect ratios, excellent mechanical strength, and electrical and thermal conductivity.[17,18] Different methods of dispersing carbon nanotubes homogenously within a polymer matrix have also been

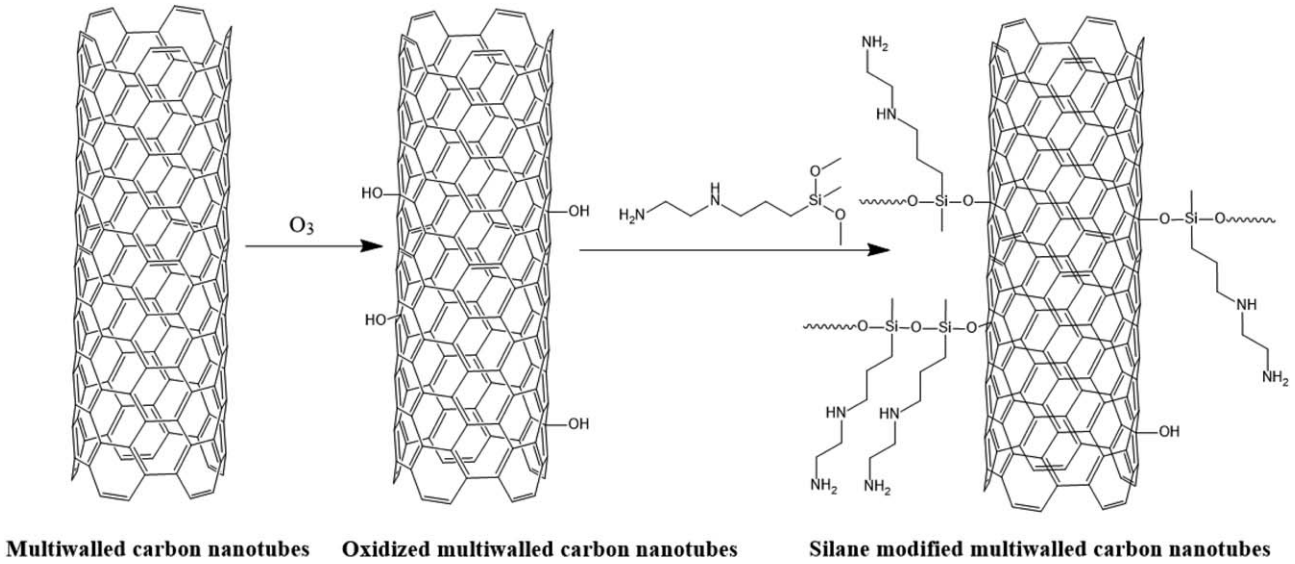

Figure 1. Modification of multiwall carbon nanotubes.

investigated. Homogeneous dispersion not only improved interfacial adhesion between the carbon nanotubes and the matrix, which is critical for load transfer, it also prevented the aggregation of carbon nanotubes, which causes heterogeneity and negatively impacts the composite's overall mechanical properties. For instance, by homogenizing 1 wt % multiwalled carbon nanotubes (MWCNTs) in a polystyrene matrix using an ultrasonic-assisted solution evaporation method, Qian reported increases in elastic modulus and tensile strength of 36–42% and 25%, respectively, which were attributed to the load transfer across the nanotube–matrix interface.[19] Similarly, using acid treatment and subsequent fluorination, Zhu discovered that the integration of 1 wt % functionalized single-walled carbon nanotubes into an epoxy matrix through strong double bonds resulted in increases of 30 and 18%, respectively, in modulus and tensile strength of the nanocomposites.[20] This was further supported by Liu, who reported that 1 wt % of terminally amino-functionalized MWCNTs increased tensile modulus of epoxy resin by 28% in a low-viscosity rubber resin system while no improvement for that in a highly viscous glassy system, which was attributed to the fact that the MWCNTs were better dispersed in former as compared to that in a highly viscous system.[21] A 370% increase in tensile strength was also reported by Kuan, who used 4 wt % amino-functionalized MWCNTs that were compatibilized with a waterborne PU matrix via ionic bonding.[22]

This paper discusses the surface modification of MWCNTs by introducing a functional amine group via ozone oxidation, followed by silanization. The amine-functionalized MWCNTs combined with isocyanates (—NCO) formed urea linkages, with residual NCO groups reacting with castor oil-based polyol, resulting in a PU matrix. Castor oil-based PU nanocomposites were thus prepared through covalent bonding between the polymer matrix and MWCNTs, with loadings ranging from 0.2 wt % to 1.2 wt %. The effect of MWCNTs loading on the thermal–mechanical properties of the PU composites were investigated.

MATERIALS AND METHODS

Materials

The polyol derived from reduced castor oil (RCP) was prepared by a reported method.[23] Polymeric diphenylmethane-4,4′-diisocyanate (PMDI, NCO content: 31 wt %) was provided by Kumho Petrochemical. Dibutyltindilaurate (DBTDL) and methyl ethyl ketone (MEK) were purchased from Sigma-Aldrich. Pristine MWCNTs (p-MWCNTs) with an average diameter of 10 nm and purities greater than 90% were supplied by Kumho Petrochemical Co. *N*-(2-aminoethyl)-3-aminopropylmethyldimethoxysilane (ADMS) was purchased from Gelest. All materials were used as received without further purification.

Fluidized Ozone Treatment and Amine Functionalized of Multiwalled Carbon Nanotubes

Multiwalled carbon nanotubes were oxidized (o-MWCNTs) to obtain primarily hydroxyl functionality using fluidized ozone treatment. Briefly, 100 mg of p-MWCNTs were placed into an empty gas purifier flask. An O_2/O_3 mixture containing 6% (wt/wt) O_3 was then flushed through the glassware from the lower insertion at a flow rate of 3 scfh, causing the MWCNTs to mix in a partially fluidized state. A porous membrane affixed to the top of the reactor allowed venting of excess gas. The gas was bubbled into iodide solution to remove any remaining O_3 before discharging into the atmosphere in a fume hood. The MWCNTs were treated for 10–90 min at a relative humidity of approx. 50%.

The amine functionalization of multiwalled carbon nanotubes (s-MWCNTs) with ADMS is shown in Figure 1. The o-MWCNTs were dispersed in Millipore water via bath sonication for 10 min. ADMS was subsequently added to the solution in a

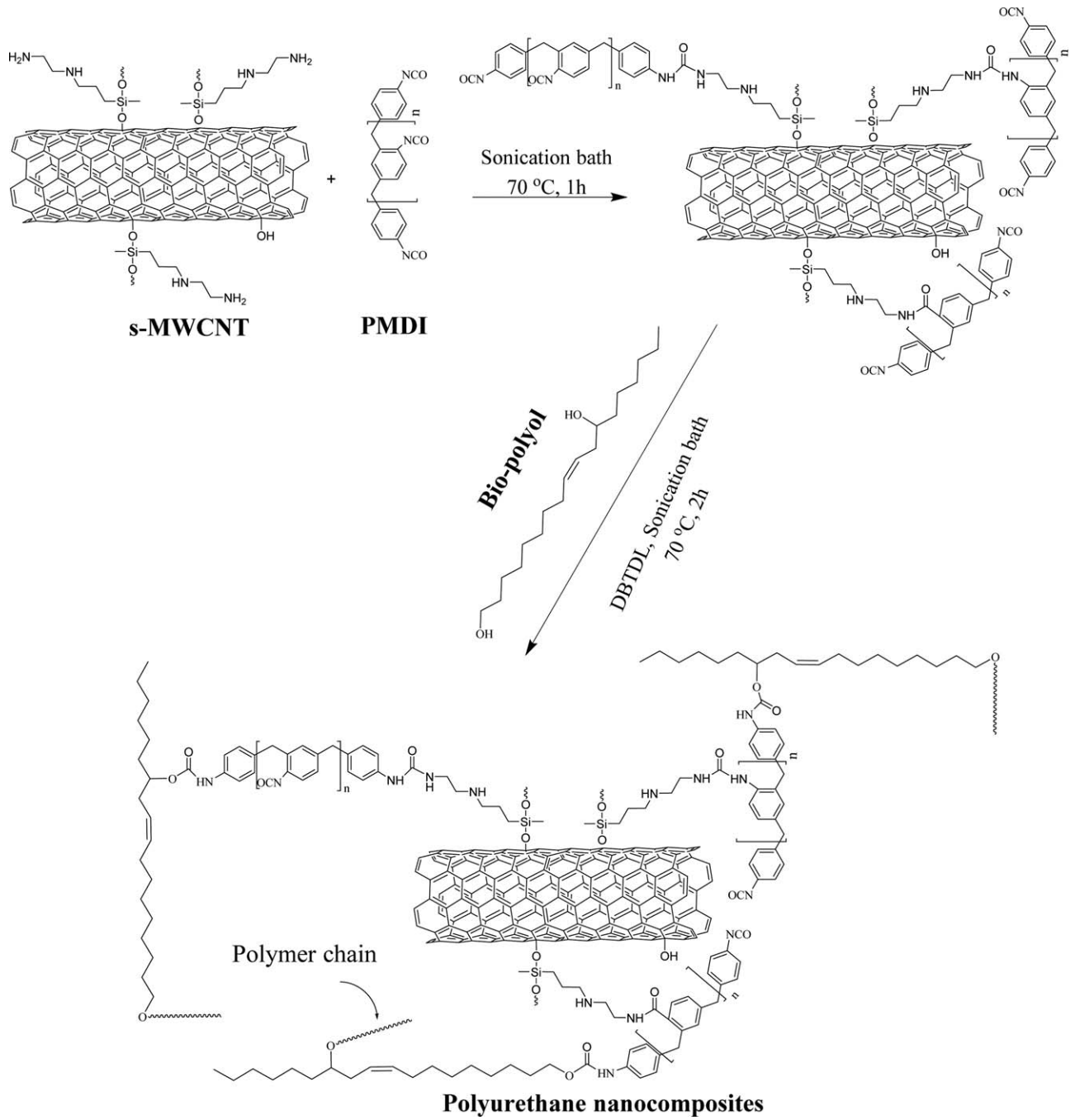

Figure 2. Schematic for the preparation of polyurethane composites.

concentration of 1.0 wt %. The solution was stirred at room temperature for 20 min, after which the MWCNTs were filtered and copiously washed with water. The resulting filtrate was heated to 110°C in an oven and held isothermally for 30 min to promote condensation of the silanols with hydroxyl groups on the nanotube surface.

Preparation of PU Nanocomposites

The preparation of PU composites is shown in Figure 2. Different loading levels of s-MWCNTs (0, 0.2, 0.4, 0.8, 1.2 wt %) were added to MEK in a small vial, and subsequently PMDI was added. The mixture was sonicated at 70°C for 1 h. Castor oil-based polyol was added and the reaction mixture was sonicated again at 70°C for 2 h. The ratio of OH in polyol to NCO in PMDI was fixed at 1 : 1.1. Then, 1% of DBTDL was added to the reaction mixture in the sonication bath for 3 min. Finally, the resulting solution was poured into a Teflon mold to form a 50 × 50 mm (length × width) sheet and postcured at 80°C overnight in an oven. The resulting PU nanocomposite films were cut into specific dimensions for thermomechanical testing.

Characterization

A Nicolet 460 Fourier transform infrared spectroscopy (FTIR) spectrometer (Madison, WI) was used to investigate the

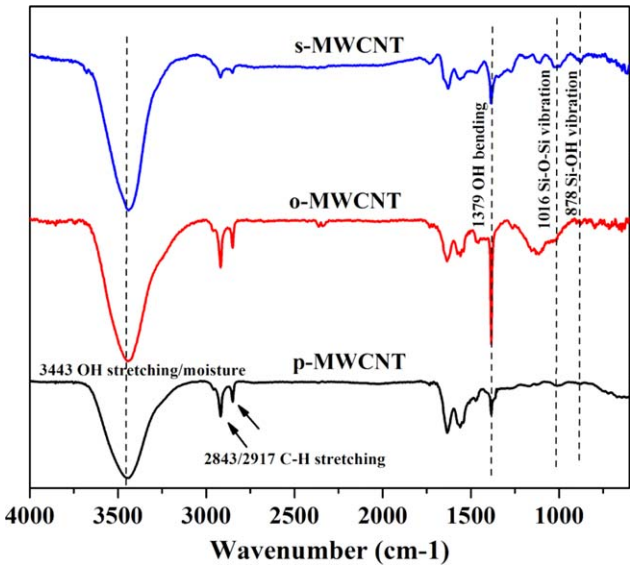

Figure 3. FTIR spectra of p-MWCNT, o-MWCNT, and s-MWCNT. [Color figure can be viewed in the online issue, which is available at wileyonlinelibrary.com.]

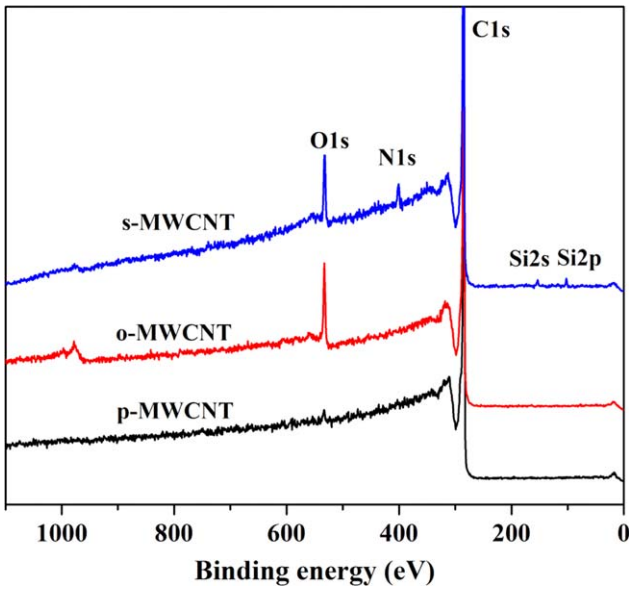

Figure 4. XPS survey scans of p-MWCNT, o-MWCNT, and s-MWCNT. [Color figure can be viewed in the online issue, which is available at wileyonlinelibrary.com.]

functional groups in p-MWCNTs, o-MWCNTs, and s-MWCNTs as well as in neat PU and the PU nanocomposites. The CNTs and polymer powder samples were pelletized with potassium bromide with a Michaelson interferometer. The elemental compositions on the surface of the CNTs were measured by X-ray photoelectron spectroscopy (XPS) using a Physical Electronics 5500 Multitechnique system with a monochromatic Al Kα radiation source. CasaXPS software was employed for data processing. The modifications on the surface of the CNTs were studied by thermogravimetric analysis (TGA, Q50, TA Instruments) in air, from room temperature to 700°C at a heating rate of 20°C/min. Samples weighing 6 mg were used for each test. The morphology of the fracture surfaces of neat PU and PU nanocomposites were investigated by scanning electron microscope (SEM, FEI Quanta 250 FEG). Transition electron microscopy (TEM) samples were cut from the nanocomposite films using an ultramicotome equipped with a diamond knife. Transmission electron micrographs were taken with a JEOL 2100 at an acceleration voltage of 200 kV.

Thermal and mechanical properties of the prepared PU nanocomposite films were characterized using a TA Instruments Q800 DMA with a film-tension mode of 1 Hz. Rectangular specimens of 0.4 × 7.0 mm (thickness × width) were used for the analysis. The samples were cooled and held isothermally for 2 min at −80°C before the temperature was increased again to 170°C at a rate of 3°C/min. The tensile properties of the PU nanocomposite films were measured using an Instron universal testing machine (model 4502) with a crosshead speed of 5 mm/min. ASTM standard dog-bone samples were used. Average values of at least three replicates of each sample were taken.

RESULTS AND DISCUSSION

Characterization of Modified Carbon Nanotubes

The change in functional groups on the surface of the carbon nanotubes after ozone and subsequent silane treatment was studied by FTIR as shown in Figure 3. The broad peak at 3443 cm^{-1} corresponds to OH stretching and ambient moisture absorbed on the surface of the CNT. The characteristic C—H stretching is shown at 2843 and 2917 cm^{-1}. The peak at 1379 cm^{-1} corresponding to OH bending increased after ozone treatment and decreased after the subsequent silane treatment. This indicated that the ozone treatment introduced new OH groups on the surface of the CNTs, while the silane treatment partially consumed the OH groups. The appearance of peaks at 1016 and 878 cm^{-1} corresponds to Si—O—Si and Si—OH vibration, thus confirming that the silane was successfully grafted on the surface of the CNTs.

Figure 4 shows the survey spectra of p-MWCNT, o-MWCNT, and s-MWCNT. The peaks at 533, 401, 286, 154, and 103 eV correspond to O1s, N1s, C1s, Si2s, and Si2p electrons, respectively.[24] Clearly, the intensities of the O1s increased significantly after ozone treatment relative to p-MWCNT. Correspondingly, the successful surface silanization of the MWCNTs reduced the relative intensity of O1s with the appearance of N1s, Si2s, and Si2p peaks.

TGA weight loss curves of p-MWCNT, o-MWCNT, and s-MWCNT are shown in Figure 5. Up to 500°C, p-MWCNTs did not show obvious weight loss, while o-MWCNTs exhibited minor weight loss caused by the decomposition of the associated organic groups.[25] For the s-MWCNTs, the comparatively low onset degradation temperature and the rapid degradation behavior in the 200–500°C temperature range are clearly a result of the grafted silane's decomposition. The higher char residue levels above 600°C are also indicative of the decomposition of the silane groups grafted on the MWCNTs' surface.

Characterization of PU Nanocomposites

The FTIR spectra of the PU nanocomposites are shown in Figure 6. The fact that the peak at 2270 cm^{-1} almost

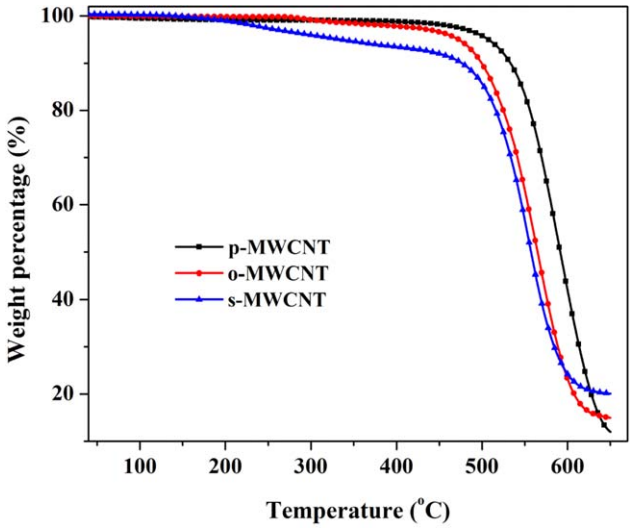

Figure 5. TGA weight loss curves of p-MWCNT, o-MWCNT, and s-MWCNT. [Color figure can be viewed in the online issue, which is available at wileyonlinelibrary.com.]

disappeared indicates that virtually all NCO groups in PMDI reacted. At the same time, the strong —NH (stretching) at 3330 cm^{-1} and the very weak —NH (stretching) at 3430 cm^{-1} indicate that most of the amine groups were involved hydrogen bonding.[26] As the s-MWCNT loading was increased, the peaks corresponding to —NH (bending) at 1530 cm^{-1} and —CN at 1228 cm^{-1} became more apparent, indicating that the amine groups in s-MWCNT reacted with the isocyanate groups.[22,27] The resulting —NH groups provided more hydrogen bonding sites to —C═O, leading to a decrease in peaks of nonhydrogen bonded —C═O at 1739 cm^{-1} and an increase of hydrogen bonded —C═O at 1710 cm^{-1}. This spectrum clearly shows that s-MWCNTs were successfully grafted into PU networks.

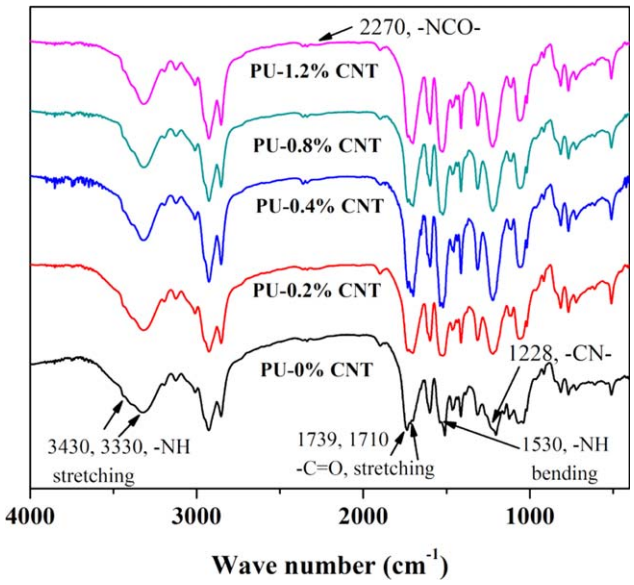

Figure 6. FTIR spectra of neat PU and PU nanocomposites (in the figure, CNT: s-MWCNT). [Color figure can be viewed in the online issue, which is available at wileyonlinelibrary.com.]

Figure 7. PU and PU/s-MWCNT nanocomposites (from left to right: with 0%, 0.2 wt %, 0.4 wt %, 0.8 wt %, 1.2 wt % s-MWCNT). [Color figure can be viewed in the online issue, which is available at wileyonlinelibrary.com.]

The nanocomposite samples turned dark with increasing s-MWCNT loading, see Figure 7. The morphologies of the PU nanocomposites were investigated by SEM as shown in Figure 8. Neat PU showed a flat fracture surface with limited river markings, resembling linear stripes, indicating brittle failure. With increasing s-MWCNT loadings in the PU matrix, the density of the river markings increased and they curved as indicated by red arrows in Figure 8(f), suggesting that the cracks deflected during propagation because of the reinforcing effect of the s-MWCNTs. As shown in Figure 8(f), the s-MWCNTs were dispersed homogenously in the matrix. However, the TEM photomicrograph of the PU nanocomposites in Figure 9 shows that the inevitable agglomeration of carbon nanotubes increased in proportion to its loading level.

Storage modulus, loss modulus, and tan δ as functions of temperature for PU nanocomposites with different levels of s-MWCNT loading are shown in Figures 10 and 11. The storage modulus values at 60°C are presented in Table I. The T_g values associated with α relaxation of both PU and its nanocomposites as determined by the peak maximum of tan δ and the loss modulus peak are also shown in Table I. All samples were initially in a glassy state, exhibiting E' values typical for polymers on the order of 1000 MPa at low temperatures. As temperatures increased to 50°C, the storage moduli of all samples decreased gradually. At temperatures above 50°C, the storage moduli of all samples plummeted, leading to the transition from the glassy to the rubbery state because of segment mobility in the crosslinked polymer networks. The addition of s-MWCNTs up to loading levels of 0.8 wt % to PU matrix resulted in a remarkable increase in storage modulus. However, an increase in s-

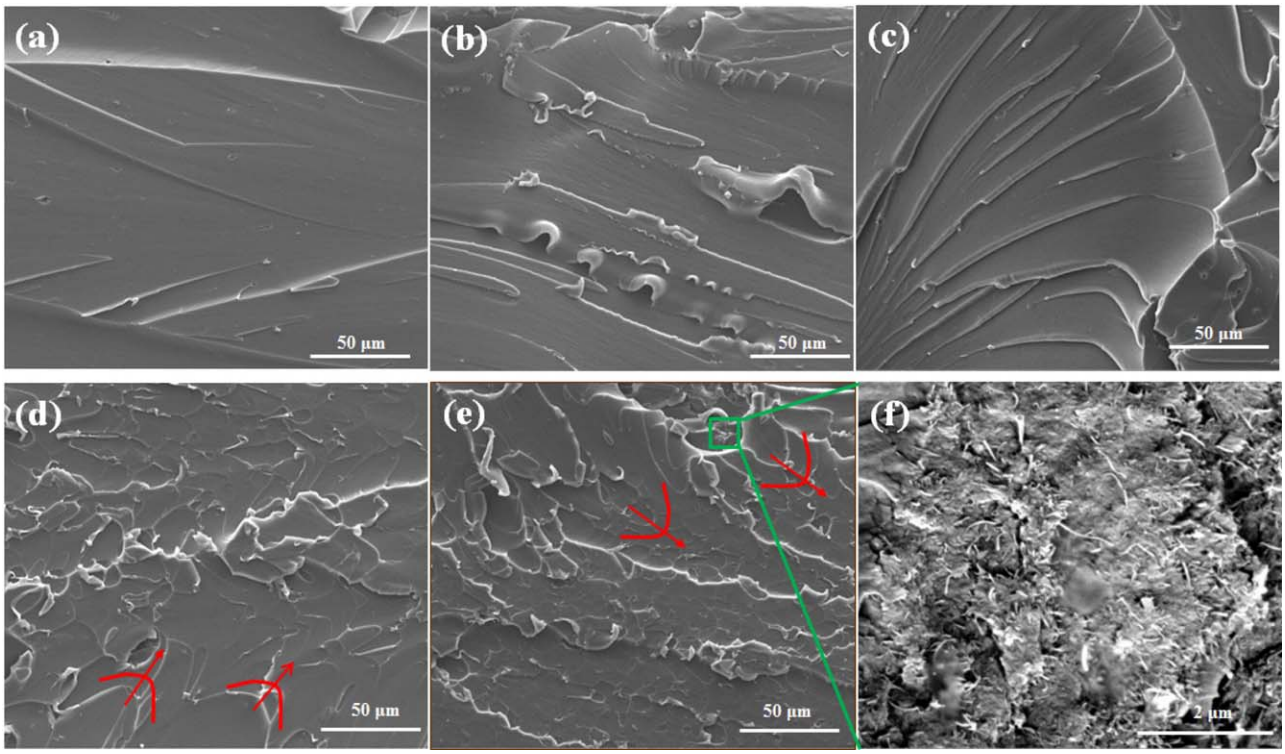

Figure 8. SEM images of the fracture surfaces of (a) neat PU, and PU nanocomposites with (b) 0.2 wt % s-MWCNT, (c) 0.4 wt % s-MWCNT, (d) 0.8 wt % s-MWCNT, (e) 1.2 wt % s-MWCNT, (f) enlarged local area of image (e). The red arrows represent the direction of the curved river markings. [Color figure can be viewed in the online issue, which is available at wileyonlinelibrary.com.]

MWCNT content to 1.2 wt % led to a decrease in storage modulus. The same trend was observed with regard to the T_gs. Also, tan δ peak maxima decreased with higher loading levels. This was attributed to an increased constraint of polymer chain movement by strong interfacial interactions. In the composites, the s-MWCNTs functioned as reinforcements, while PU served as the matrix. The incorporation of s-MWCNTs (at low loading levels) in the PU network stiffened the polymer and constrained the polymer chains, leading to enhanced storage moduli and T_g. However, as s-MWCNT loading levels reached 1.2%, excessive amine groups from s-MWCNTs competed with the polyol's hydroxyl groups for isocyanate groups as long as the ratio of NCO : OH was fixed at 1.1 : 1. This compromised the integrity of the film and resulted in decreased thermomechanical

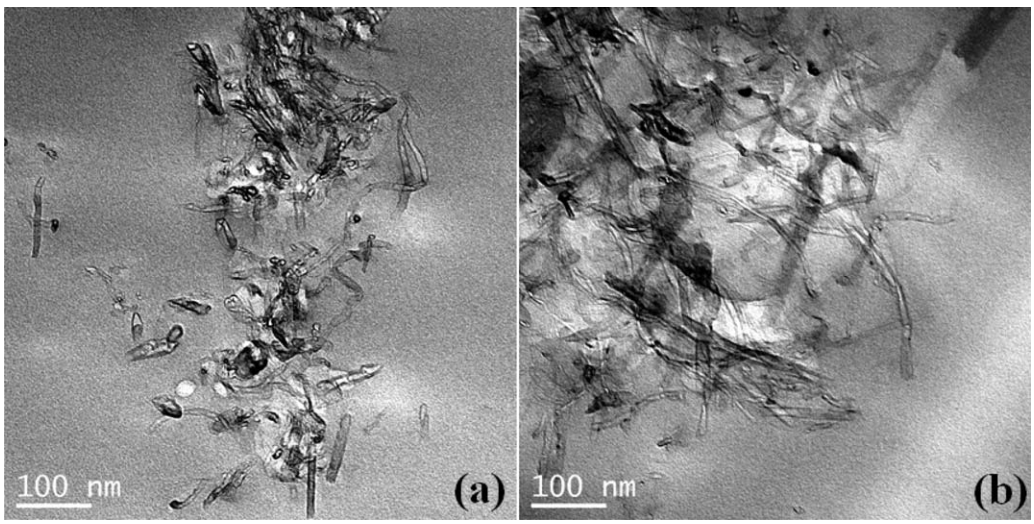

Figure 9. TEM image of PU nanocomposites with (a) 0.4 wt % s-MWCNT and (b) 1.2 wt % s-MWCNT.

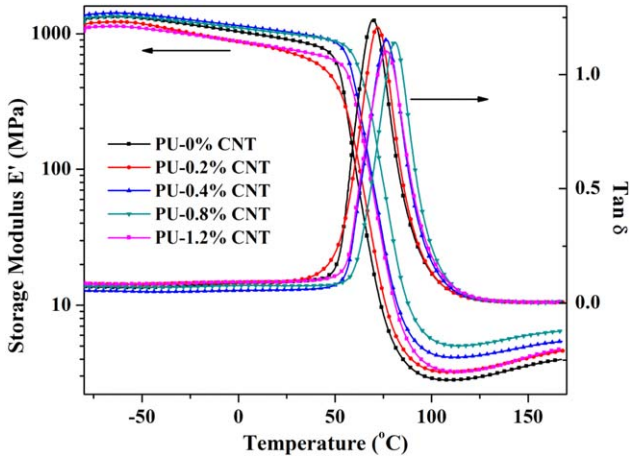

Figure 10. Temperature dependence of storage modulus and tan δ for PU and PU/s-MWCNT nanocomposites (in the figure, CNT: s-MWCNT). [Color figure can be viewed in the online issue, which is available at wileyonlinelibrary.com.]

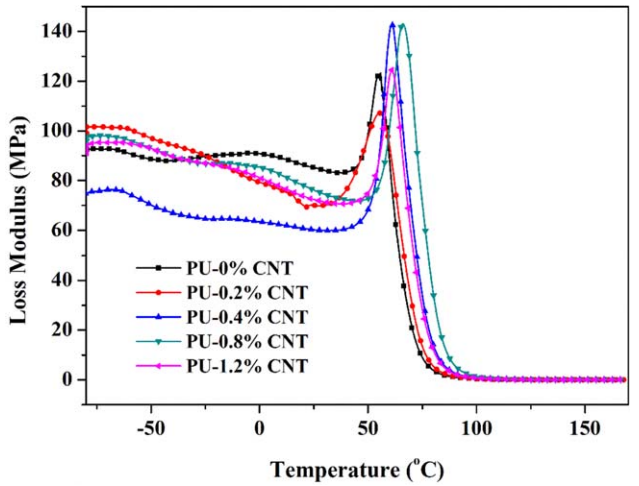

Figure 11. Temperature dependence of loss modulus for PU and PU/s-MWCNT nanocomposites (in the figure, CNT: s-MWCNT). [Color figure can be viewed in the online issue, which is available at wileyonlinelibrary.com.]

properties. Also, the lower values of storage modulus and T_g for nanocomposites with s-MWCNT loading levels above 8 wt % were attributed to the inevitable aggregation of the nanotubes at high contents. Similar results were reported by Liu for epoxidized soybean oil/clay nanocomposites.[28]

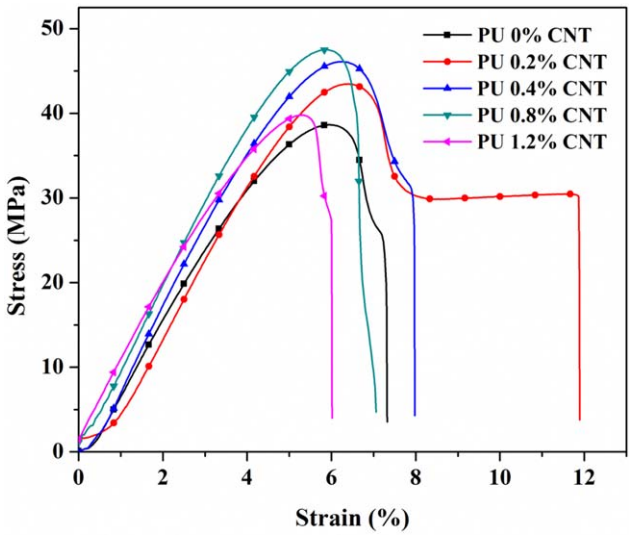

Figure 12. Stress–strain curves of PU and PU/s-MWCNT nanocomposites (in the figure, CNT: s-MWCNT). [Color figure can be viewed in the online issue, which is available at wileyonlinelibrary.com.]

Figure 12 shows the stress–strain curves of PU and the PU/s-MWCNT nanocomposites. The tensile strength, elongation at break, and Young's modulus are summarized in Table I. As s-MWCNT loading increased from 0 to 0.8%, the tensile strength of the nanocomposite films increased by 22% from 39.1 to 47.8 MPa. Similarly, a steady rise in Young's modulus and decrease in elongation at break were observed. The increase in mechanical properties of the PU nanocomposites was attributed to the reinforcing effect of the CNTs, which constrained motion of the polymer chains and favored efficient load transfer from the matrix to the s-MWCNTs.[29] However, as the s-MWCNT loading level increased to 1.2%, tensile strength and Young's modulus decreased.

CONCLUSIONS

The CNTs were surface functionalized by amine groups via ozone oxidation followed by silanization. The amine functionalized CNTs were incorporated into castor oil-based PU matrices via strong covalent bonding. It was possible to disperse the CNTs effectively and improve the interfacial strength between them and the polymer matrix. The thermomechanical properties (storage modulus, glass transition temperature, Young's modulus, and tensile strength) of the PU nanocomposites increased with increasing CNT loadings up to 0.8%. When

Table I. Properties of PU Nanocomposites

	Storage modulus (MPa) at 60°C	T_g (°C) (tan δ/loss modulus)	Tensile strength (MPa)	Elongation at break (%)	Young's modulus (MPa)
PU-0% s-MWCNT	115	69.6/55.8	39.1 ± 0.6	6.5 ± 1.0	1000.8 ± 5.7
PU-0.2% s-MWCNT	157	71.9/56.1	44.3 ± 1.1	10.6 ± 1.9	1043.5 ± 20.7
PU-0.4% s-MWCNT	428	76.6/61.1	46.4 ± 0.4	8.0 ± 0.3	1100.4 ± 37.3
PU-0.8% s-MWCNT	661	81.0/66.4	47.8 ± 0.8	7.0 ± 0.4	1102.8 ± 17.2
PU-1.2% s-MWCNT	340	76.7/60.9	43.4 ± 3.8	6.3 ± 0.3	1039.3 ± 75.2

nanotube loadings increased to 1.2%, the properties of the PU nanocomposites decreased because a high number of amine groups present in high loadings of CNTs competed for the isocyanate groups with the hydroxyl groups in the polyol, compromising the integrity of the PU matrix. High loading levels of CNTs also led to nanotube agglomeration, which negatively affected the thermomechanical properties of the nanocomposites.

ACKNOWLEDGMENTS

Partial funding from the National Science Foundation (under Grant No. CMMI1348747) is gratefully acknowledged.

REFERENCES

1. Petrovic, Z. S. *Polym. Rev.* **2008**, *48*, 109.
2. Xia, Y.; Larock, R. C. *Green Chem.* **2010**, *12* 1893.
3. Ionescu, M. Chemistry and Technology of Polyols For Polyurethanes; Rapra Technology: Shawbury, Shrewsbury, Shropshire, U.K., **2005**.
4. Pfister, D. P.; Xia, Y.; Larock, R. C. *ChemSusChem* **2011**, *4*, 703.
5. Zhang, L.; Jeon, H. K.; Malsam, J.; Herrington, R.; Macosko, C. W. *Polymer* **2007**, *48*, 6656.
6. Williams, C. K.; Hillmyer, M. A. *Polym. Rev.* **2008**, *48*, 1.
7. Desroches, M.; Escouvois, M.; Auvergne, R.; Caillol, S.; Boutevin, B. *Polym. Rev.* **2012**, *52*, 38.
8. Zhang, C. Q.; Xia, Y.; Chen, R. Q.; Huh, S.; Johnston, P. A.; Kessler, M. R. *Green Chem.* **2013**, *15*, 1477.
9. Lu, Y. S.; Larock, R. C. *ChemSusChem* **2010**, *3*, 329.
10. Lligadas, G.; Ronda, J. C.; Galia, M.; Cadiz, V. *Biomacromolecules* **2007**, *8*, 686.
11. Guo, A.; Javni, I.; Petrovic, Z. *J. Appl. Polym. Sci.* **2000**, *77*, 467.
12. Husic, S.; Javni, I.; Petrovic, Z. S. *Compos. Sci. Technol.* **2005**, *65*, 19,
13. Merlini, C.; Ramoa, S. D. A. S.; Barra, G. M. O. *Polym. Composite Compos.* **2013**, *34*, 537.
14. Merlini, C.; Soldi, V.; Barra, G. M. O. *Polym. Test* **2011**, *30*, 833.
15. Dwan'isa, J. P. L.; Mohanty, A. K.; Misra, M.; Drzal, L. T.; Kazemizadeh, M. *J. Mater. Sci.* **2004**, *39*, 2081.
16. Dong, K.; Qiu, F. X.; Guo, X. R.; Xu, J. C.; Yang, D. Y.; He, K. C. *J. Appl. Polym. Sci.* **2013**, *129*, 1697.
17. Calvert, P. *Nature* **1999**, *399*, 210.
18. Kashiwagi, T.; Grulke, E.; Hilding, J.; Harris, R.; Awad, W.; Douglas, J. *Macromol. Rapid Commun.* **2002**, *23*, 761,
19. Qian, D.; Dickey, E. C.; Andrews, R.; Rantell, T. *Appl. Phys. Lett.* **2000**, *76*, 2868.
20. Zhu, J.; Kim, J. D.; Peng, H. Q.; Margrave, J. L.; Khabashesku, V. N.; Barrera, E. V. *Nano Lett.* **2003**, *3*, 1107.
21. Liu, L. Q.; Wagner, H. D. *Compos. Sci. Technol.* **2005**, *65*, 1861.
22. Kuan, H. C.; Ma, C. C. M.; Chang, W. P.; Yuen, S. M.; Wu, H. H.; Lee, T. M. *Compos. Sci. Technol.* **2005**, *65*, 1703.
23. Zhang, C. Q.; Ding, R.; Kessler, M. R. *Macromol. Rapid Commun.* **2014**, *35*, 1068.
24. Peng, K.; Liu, L. Q.; Li, H. C.; Meyer, H.; Zhang, Z. *Carbon* **2011**, *49*, 70.
25. Abuilaiwi, F. A.; Laoui, T.; Al-Harthi, M.; Atieh, M. A. *Arab J. Sci. Eng.* **2010**, *35*, 37.
26. Lu, Y. S.; Larock, R. C. *Biomacromolecules* **2008**, *9*, 3332.
27. Wang, T. L.; Yu, C. C.; Yang, C. H.; Shieh, Y. T.; Tsai, Y. Z.; Wang, N. F. *J. Nanomater.* **2011**, *2011*, 9 pp. Article ID 814903. DOI:10.1155/2011/814903
28. Liu, Z. S.; Erhan, S. Z.; Xu, J. Y. *Polymer* **2005**, *46*, 10119,
29. Yan, D. X.; Xu, L.; Chen, C.; Tang, J. H.; Ji, X.; Li, Z. M. *Polym. Int.* **2012**, *61*, 1107.